

Thermodynamic Parameters for the Adsorption of Aromatic Hydrocarbon Vapors at the Gas–Water Interface

Suresh Raja, Frank S. Yaccone, Raghunathan Ravikrishna, and Kalliat T. Valsaraj*

Gordon A. and Mary Cain Department of Chemical Engineering, Louisiana State University, Baton Rouge, Louisiana 70803-7303

Experimental data on the adsorption of polycyclic aromatic hydrocarbons (PAHs) at the gas–water interface is lacking. The inverse gas chromatography (IGC) technique with Chromosorb P NAW as the packing support was used to obtain the thermodynamic parameters for the adsorption of three aromatic compounds (benzene, naphthalene, and phenanthrene) at the gas–water interface. The partition constants at different temperatures were measured and used to compute the free energy, enthalpy, and entropy of adsorption using the Gibbs–Helmholtz equation. The enthalpy of adsorption at the gas–water interface for all three compounds was larger than the enthalpy of condensation and the enthalpy of aqueous solvation. This supports the prevailing “critical cluster” model for the dynamics of the transfer of compounds to the gas–water interface. The thermodynamics of adsorption at the gas–solid interface was more favorable than that at the gas–water interface. The partition constant at the gas–water interface was correlated with the subcooled liquid vapor pressure of the PAHs. The possible effect of gas–water partitioning of PAHs upon their wet deposition from the atmosphere is explored theoretically.

Introduction

Gas–water and gas–solid interfaces play significant roles in the fate and transport of contaminants in the environment. There is ample documented evidence that organic contaminants are transported in the atmosphere over local, regional, and global scales via “wet” and “dry” deposition. Atmospheric scientists have studied these issues in considerable detail. At the gas–water interface emphasis has been on the equilibrium properties between the bulk gas and water phases as given by Henry’s law.¹ However, it has been pointed out that, in those cases where one phase is dispersed in the other as an assemblage of finely divided entities, the gas–water interface becomes more important than the two bulk phases.² Examples are small air bubbles in water, mist, and fog droplets in air. At the gas–solid interface, the surface areas of finely divided particles (e.g., aerosols) play a large role in the transport of contaminants. It is known that, at the gas–solid interface, the presence of water influences the partitioning of contaminants to the interface.³

Of the myriad organic compounds found in the environment, one important class is the polycyclic aromatic hydrocarbons (PAHs) present in the air.⁴ PAHs are of two types, the biaryls and the condensed benzenoid hydrocarbons, the latter being the larger and more important group. The condensed benzenoid compounds are characterized by two or more benzene rings fused at ortho positions so that each pair of rings shares two carbon atoms. They are produced during pyrolysis and combustion of organic matter, fossil fuels, and petrochemicals, sedimentary organic matter generation, and even biosynthesis by organisms. PAHs are the most abundant class of carbon-bearing compounds in the universe.⁵ PAHs are hydrophobic and hence accumulate in organic rich environments such as lipids, aerosols, and soil particles. Some of them are

suspected carcinogens, and hence their environmental fates in aerosols and atmospheric moisture have been topics of much study. They are also ubiquitous in contaminated sediments and soil. Work done in our laboratory characterized their presence in the metro Baton Rouge atmosphere.⁶

A large body of literature exists on the exchange of PAHs between the aquatic and air environments. The bulk phase partitioning between air and water has been studied extensively; however, only recently has the behavior at the gas–water interface been a focus of attention.^{7–11} Over many decades starting in the 1920s, there have been considerable studies on the adsorption of organic vapor to thin films of water.^{12–21} The current theory regarding the dynamics of the entry of molecules from the gas to the water phase is based on the “critical cluster” model proposed by Davidovits and co-workers.²² This model presumes that the gas–water interface is a dynamic region where aggregates are continually forming, dissipating, and reforming. As gas molecules enter this region, they are adsorbed at the interface from where they are partially solvated via cluster formation with water molecules. Thereupon, they are incorporated into the bulk solution phase when the cluster reaches a critical size. The interfacial adsorption of vapor phase compounds in environmental systems is, therefore, an important subject.²³ The importance of gas–liquid interfacial adsorption of organic compounds in fog droplets, water in thin films in the vadose zone, and air bubbles in flotation and microlayer enrichment in the seawater environment is recognized.^{24–28}

Few, if any, experimental data exist on the gas–water interfacial binding of semivolatile organic compounds, such as PAHs. Presently, only theoretical correlations are available to fill this gap of information. In this paper we report our data on the adsorption of benzene, naphthalene, and phenanthrene at the gas–water interface from the vapor phase. The inverse gas chromatography (IGC) technique was used to measure the adsorption on dry and water-coated Chromosorb P. The data were used to obtain the

* Author for correspondence. Phone: 225 578 6522. Fax: 225 578 1476. E-mail: valsaraj@che.lsu.edu.

Table 1. Physicochemical Properties of the Aromatic Hydrocarbons Used in the Experiments^{36–38}

property	benzene	naphthalene	phenanthrene
molecular weight	78	128	178
aqueous solubility/mol·m ⁻³	23	0.241	0.006 17
subcooled liquid vapor pressure, $P_{s(0)}/\text{kPa}$	12.7	0.037	9×10^{-5}
enthalpy of condensation, $\Delta^{\text{L}}H/\text{kJ}\cdot\text{mol}^{-1}$	-34	-58	-75
enthalpy of solvation, $\Delta_{\text{solv}}H^{\text{E}}/\text{kJ}\cdot\text{mol}^{-1}$	-31	-47	-54

value of the binding constant for the compounds at the gas–water interface. The effects of water contents and temperature on the adsorption are studied. The enthalpy data on adsorption were obtained and correlated with the solvation energies. The adsorption constants were correlated to the subcooled liquid vapor pressures of a large number of PAH compounds.

Experimental Section

Theory and Methodology. There are basically two methods for determining the values of the partition constants of vapors to the gas–water interface. They fall into two categories: (a) static surface pressure measurements that rely on the determination of the change of surface tension of a clean water interface as it contacts vapors (The method is limited to compounds with large vapor pressures but is extremely susceptible to surface impurities.^{14,16,29,30}) and (b) an inverse gas chromatography (IGC) method that relies on determining the chromatographic retention times of vapors passed over a water-coated adsorbent.^{18–20,24,31} IGC is far more suitable for compounds with low vapor pressure such as the PAHs and is particularly suitable to study temperature effects on adsorption.

IGC is different from conventional GC in that the stationary phase is the analyte. The mobile phase (gas) is used to introduce probes of known characteristics, and the output (retention time and peak shape) is used to obtain information about the stationary phase. In the present case, a water-coated packing is used to retain the compound (probe) of interest. The overall retention of the probe is due to bulk phase partitioning into the water film as well as the adsorption on the gas–water interface of the water film. The net retention volume per gram of adsorbent is given by

$$V_N = K_{\text{IA}}A_W + K_{\text{WA}}V_W \quad (1)$$

where V_N , A_W , and V_W are respectively the total retention volume, specific gas–water interface area, and volume of water per unit mass of adsorbent. K_{IA} is the equilibrium ratio of the adsorbed concentration, Γ_i , to the vapor concentration, C_a , and K_{WA} is the molar concentration ratio of the bulk aqueous phase concentration to the vapor concentration.

Experimentally, the net retention volume is obtained from $K_c V_M$, where K_c is the capacity factor and V_M is the volume of gas-phase per unit mass of adsorbent. In turn, the capacity factor is obtained from $K_c = (t_R/t_M - 1)$, where t_R is the retention time of the probe and t_M that of a nonretained tracer (methane). Thus, by plotting V_N/V_W against A_W/V_W , the value of K_{IA} can be determined from the slope. V_W is obtained from the volume of water added to the column during preparation, while A_W is obtained from the net retention volume of heptane by assuming that the partitioning in bulk water is negligible, as demonstrated by others.^{18,24} The specific surface areas ranged from (12 500 to 50 000) cm²·g⁻¹ for the ranges of specific water volumes used in this series of experiments. The experiments were repeated for different temperatures to obtain K_{IA} as a function of temperature. Temperature was

controlled by the gas chromatograph oven temperature control panel.

Experimental Apparatus and Procedure. The compounds considered were benzene (99.9%, Fisher Scientific Company), naphthalene (99.9%, Fisher Scientific Co.), and phenanthrene (98%, Aldrich Chemical Co.). The physicochemical properties of the compounds are given in Table 1. No influence of impurities that might be surface active was detected in this work. Samples of the compound were obtained from the vapor phase in a closed bottle containing the pure compound that was maintained in a temperature-controlled bath. A gastight syringe was used to obtain the required amount of the vapor sample from the bottle and inject it onto the test column. Sample sizes injected ranged from (1×10^{-7} to 2×10^{-7}) m³ for benzene and 5×10^{-7} m³ and higher for naphthalene and phenanthrene because of their low vapor pressures. These amounted to less than 10^{-5} mole fraction at the outlet, so as to avoid column overloads.

The vapor stream entered a Hewlett-Packard gas chromatograph (HP 5890A) that contained a stainless steel column (0.91 m \times 0.006 35 m i.d.) packed with Chromosorb P obtained from Supelco Inc. Chromosorb P is a non-acid-washed, porous diatomaceous support. The packing had a surface area of (4 to 5) m²·g⁻¹, a bulk density of 0.38 g·cm⁻³, and a mean particle density of 2.3 g·cm⁻³. The carrier gas (helium) flow rate was approximately 5×10^{-5} m³·min⁻¹ with inlet pressure maintained at 152 kPa, and the outlet pressure was atmospheric. Presaturation of helium with water before entering the column prevented column bleed. The compounds were detected at the outlet of the column using a flame ionization detector (FID), and the retention times (t_R) were recorded. The experiment was conducted in an isothermal mode and repeated for different column temperatures at constant flow rates. At each temperature, experiments were also repeated for different water contents in the column.

Column Packing Procedure. The packing material was washed thoroughly with HPLC grade water and dried in an oven overnight and cooled in a desiccator. The clean, dry material was loaded with a measured quantity of distilled, deionized HPLC grade water. The mass of water loaded was checked by weighing samples of the material and drying them at 100 °C for about 6 h. However, water loss during loading of the column using gentle suction did occur. Hence, the samples were weighed before and after experiments to obtain an estimate of the actual amount of water in the column. The water loading ranged from (0.036 to 0.38) mass of water per unit mass of support.

Results and Discussion

Thermodynamics of Adsorption at the Gas–Water Interface. We begin with the criteria of equal chemical potentials for the substances in the bulk gas phase and at the gas–water interface with which it is at equilibrium. Thus, we have the following equation

$$\mu_i^{\text{g}} + RT \ln \left(\frac{P_i}{P_i^{\circ}} \right) = \mu_i^{\text{w}} + RT \ln \left(\frac{\gamma_i^{\text{w}} \pi_i}{\pi_i^{\circ}} \right) \quad (2)$$

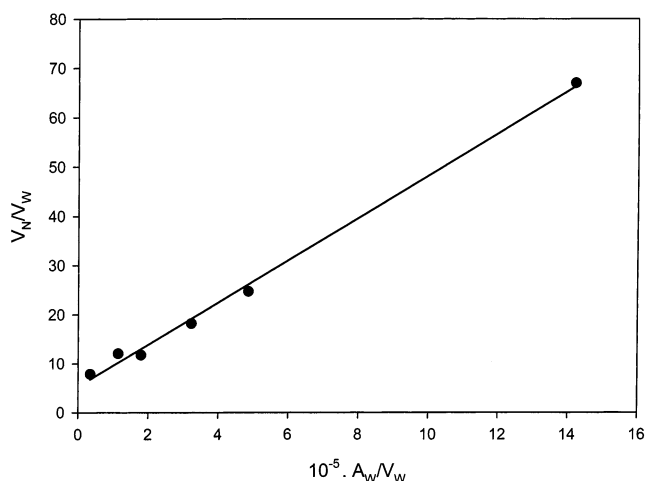


Figure 1. Plot of V_N/V_W versus A_W/V_W for benzene at 298 K ($r^2 = 0.996$).

where $P_i^\circ = 101.325$ kPa is the standard state pressure for the gas phase, $\pi_i^\circ = 0.06084$ mN·m⁻¹ is the corresponding standard state surface pressure proposed by Kemball and Rideal,³² and γ_i^σ is included to consider nonideality in the surface phase. The surface activity coefficient is an unknown function of the surface coverage or surface pressure, π_i . However, as defined, $\gamma_i^\sigma \rightarrow 1$ as $\pi_i \rightarrow 0$. Therefore, the standard state Gibbs free energy for the transfer of the molecule from the bulk air to the air–water interface is given by

$$\Delta G_{\text{IA}}^\circ = -RT \ln \left(\frac{\pi_i}{P_i} \frac{1}{\delta_0} \right) \quad (3)$$

where δ_0 is the ratio of the standard states or otherwise called the standard surface thickness ($=6 \times 10^{-10}$ m). Since the equation of state for the two-dimensional gaseous state is similar to that for the ideal gaseous state for the bulk phase, the ratio π_i/P_i is the same as the ratio $\Gamma_i/C_A = K_{\text{IA}}$, the surface adsorption equilibrium constant. Thus

$$\Delta G_{\text{IA}}^\circ = -RT \ln \left(\frac{K_{\text{IA}}}{\delta_0} \right)$$

The enthalpy of adsorption is obtained from the temperature variation of the free energy as per the Gibbs–Helmholtz equation:

$$\frac{d}{dT} \left(\ln \frac{K_{\text{IA}}}{\delta_0} \right) = \frac{\Delta H_{\text{IA}}^\circ}{RT^2} \quad (4)$$

The entropy of adsorption is obtained from $\Delta S_{\text{IA}}^\circ = (1/T)(\Delta H_{\text{IA}}^\circ - \Delta G_{\text{IA}}^\circ)$.

Adsorption at the Gas–Water Interface of Water-Coated Chromosorb P NAW. Adsorption of the vapor occurs on the gas–water interface of the support with a simultaneous dissolution in the bulk water present on the surface.¹⁸ Equation 1 can be rewritten as eq 5 below.

$$\frac{V_N}{V_W} = K_{\text{WA}} + K_{\text{IA}} \frac{A_W}{V_W} \quad (5)$$

Figure 1 is an example of the applicability of the above equation for benzene at 298 K, where V_N/V_W is plotted against A_W/V_W . The value of K_{IA} for benzene obtained at 298 K was $0.43 \mu\text{m}$. The value of K_{WA} obtained for benzene was 5.2. The experiment was repeated for different tem-

peratures to obtain the temperature variation of K_{IA} . Similar plots were made for naphthalene and phenanthrene at different temperatures. Linearity of the adsorption isotherm was ascertained by varying the vapor concentrations of the compound injected onto the inlet of the GC column. No significant variations in peak shape or retention times were observed over the concentration ranges investigated in this work.

Table 2 lists the values of K_{IA} and $\Delta G_{\text{IA}}^\circ$ obtained from Figure 2 for benzene, naphthalene, and phenanthrene at 298 K. The value of K_{IA} obtained for benzene in this work at 298 K is in excellent agreement with other reported values in the literature, as shown in Table 2. The value of $\Delta G_{\text{IA}}^\circ$ obtained from this work for benzene was (-16.3 ± 0.04) kJ·mol⁻¹. This is also in excellent agreement with the value of -16.3 kJ·mol⁻¹ at 298 K reported recently by Braunt and Conklin³⁵ using axisymmetric drop shape analysis. More important is the agreement with the theoretical value of (-16.6 ± 1.6) kJ·mol⁻¹ reported by Dang and Feller³⁹ using molecular dynamics calculations of the water–benzene interactions at the gas–water interface. The molecular dynamics calculations revealed that the benzene orientation was parallel to the interface when the molecule was located at the minimum of the free energy profile. There is ample evidence from spectroscopy in the recent literature that benzene is capable of weakly hydrogen bonding with water through its delocalized π -electrons.⁴⁰ Evidence points to a clear orientation of the two H atoms of water pointed toward the π cloud of the benzene plane. To the best of our knowledge, there are presently no reported or calculated values in the literature for the free energy and partition constant for the adsorption of naphthalene and phenanthrene at the gas–water interface. The K_{IA} value for naphthalene obtained at 298 K is nearly 80 times larger than that for benzene, and the adsorption free energy for naphthalene at 298 K is 1.6 times larger than that for benzene. If, as indicated for benzene, naphthalene is also adsorbed parallel to the surface, the adsorption free energy should be proportional to the molecular surface area. Thus, since the area of a benzene molecule is 110 \AA^2 and that of the naphthalene is 156 \AA^2 , the adsorption free energy of naphthalene is expected to be 1.4 times larger.

Figure 2 shows plots of $\ln(K_{\text{IA}}/\delta_0)$ as a function of $1/T$ for benzene, naphthalene, and phenanthrene. From the slopes of these plots, the values of $\Delta H_{\text{IA}}^\circ$ and $\Delta S_{\text{IA}}^\circ$ for each compound can be obtained. These values are shown in Table 2. Also shown in Table 2 are the literature reported values for benzene. To the best of our knowledge, no other values are presently available in the literature for the enthalpy and entropy of adsorption of naphthalene and phenanthrene. To calculate $\Delta H_{\text{IA}}^\circ$ for benzene, we included the value of K_{IA} obtained by Karger et al.¹⁸ at 12.5°C along with our values from $(25$ to $45)^\circ\text{C}$. The straight line plot and the goodness of fit show that extrapolation over a wide temperature range is possible and that $\Delta H_{\text{IA}}^\circ$ is a constant over the temperature range from $(12.5$ to $45)^\circ\text{C}$. Similar arguments also apply for naphthalene. The heat of adsorption obtained for naphthalene is 26 kJ·mol⁻¹ larger than that for benzene, and that for phenanthrene is 37 kJ·mol⁻¹ larger than that for naphthalene. Whereas the errors involved in the measured values of thermodynamic quantities for benzene and naphthalene are relatively small, that for phenanthrene is somewhat large because of the difficulties in obtaining reproducible vapor samples at high temperatures.

Table 2. Thermodynamic Parameters for the Adsorption of Aromatic Hydrocarbons at the Gas–Solid and Gas–Liquid Interfaces and Standard Deviations of the Measured Values^a

property	benzene	naphthalene	phenanthrene
	Parameters for the Gas–Solid Interface		
$\Delta H_{SA}^{\circ}/\text{kJ}\cdot\text{mol}^{-1}$	-45 ± 2	-80 ± 2	-116.1 ± 0.3
$\Delta S_{SA}^{\circ}/\text{J}\cdot\text{K}^{-1}\cdot\text{mol}^{-1}$	-73 ± 1	-95 ± 5	-152 ± 5
	Parameters for the Gas–Liquid Interface		
$K_{IA}/\mu\text{m}$ at 298 K	0.43 \pm 0.01 (this work) 0.49 (ref 24) 0.41 (ref 35) 0.44 (ref 24)	27.2 \pm 1.8	1×10^5
$\Delta G_{IA}^{\circ}/\text{kJ}\cdot\text{mol}^{-1}$ at 298 K	-16.3 ± 0.04	-26.5 ± 0.1	-46
$\Delta H_{IA}^{\circ}/\text{kJ}\cdot\text{mol}^{-1}$	-41 ± 2 (this work) -41 (ref 35) -26 (ref 20) -31 (ref 15) -31 (ref 40 – theory) -32 (ref 42 – theory)	-67 ± 17	-104 ± 36
$\Delta S_{IA}^{\circ}/\text{J}\cdot\text{K}^{-1}\cdot\text{mol}^{-1}$	-82 ± 4 (this work) -83 (ref 35) -50 (ref 20)	-135 ± 56	-195 ± 120

^a Uncertainties for K_{IA} are based on standard errors on the linear regression of V_N/V_W versus A_l/V_W curves as in Figure 1. Uncertainties for ΔH_{IA}° and ΔS_{IA}° are based on standard errors for the linear regression on the integral form of the Gibbs–Helmholtz equation as shown in Figure 2. All standard errors are based on 95% confidence limits based on the Student's t-test.

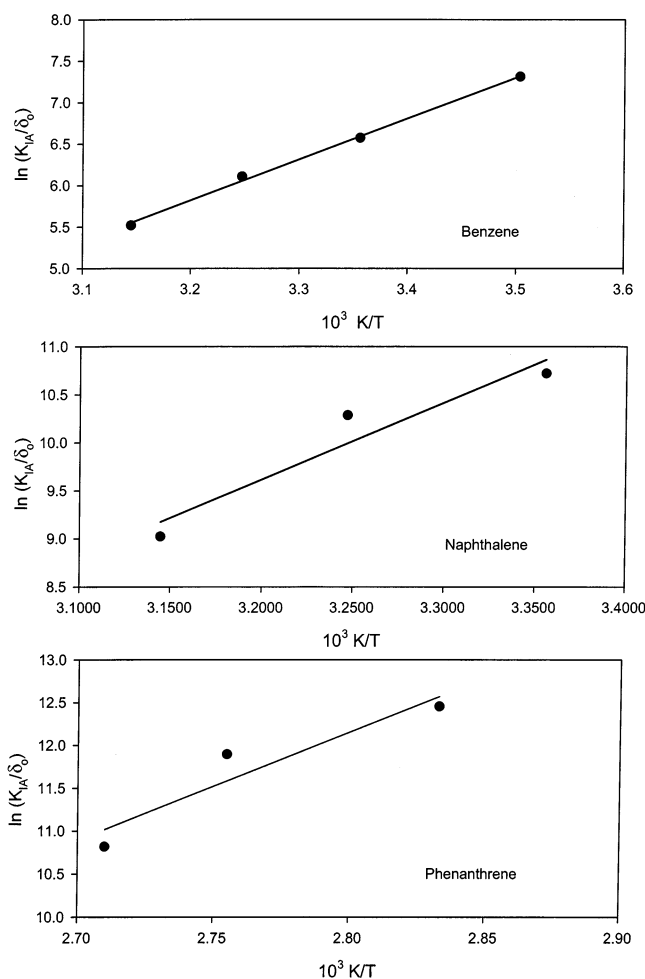


Figure 2. Integral form of the Gibbs–Helmholtz equation for benzene ($r^2 = 0.998$), naphthalene ($r^2 = 0.936$), and phenanthrene ($r^2 = 0.892$) at the gas–water interface.

Table 1 also lists the enthalpy of condensation (liquefaction) and enthalpy of solvation from the gas phase for the PAHs considered in this work. Comparison with the heat of condensation ($\Delta_g H^{\circ}$) showed larger enthalpy of adsorption for benzene, naphthalene, and phenanthrene at the

gas–water interface. Orem and Adamson⁴¹ reported larger enthalpy of adsorption than that of condensation of organic vapors on water at low surface coverage compared to high surface coverage. For the adsorption of alcohols, acids, and acetone at the gas–water interface, larger enthalpies of adsorption than those of condensation have been observed.⁴² The larger enthalpy of adsorption than that of condensation at low surface coverage has been explained to be because of local structuring of water molecules around organic molecules.⁴¹ This translates to stronger adsorbate–adsorbent (water) intermolecular interactions than those between the adsorbate molecules at the gas–water surface. Comparison of the enthalpy of aqueous solvation ($\Delta_{\text{solv}} H^{\circ}$) also showed large enthalpies of adsorption for the compounds. This also indicates preferential interaction with water, rather than adsorbate molecules. These observations support the “critical cluster” model of solvation described earlier,^{22,44} in which the primary assumption is that the first step in gas-to-liquid transfer involves the adsorption to the water surface through specific chemical forces, viz., the formation of a nascent solvation shell. In other words, the gas-to-liquid transfer is not a simple condensation process.

A series of runs was also made on the dry column to ascertain the binding of vapor phase PAHs to the gas–solid interface. In this case, eq 1 can be applied by neglecting the partitioning into the bulk water and using the surface area A_s of the dry packing in the place of A_w . Thus, we can obtain K_{SA} , the solid–gas partition constant for the solute. Table 2 lists the enthalpy (ΔH_{SA}°) and entropy (ΔS_{SA}°) of adsorption at the gas–solid interface. The enthalpy change per aromatic ring is approximately $-35 \text{ kJ}\cdot\text{mol}^{-1}$. A similar trend was observed for the adsorption of PAHs on dry soil. De Seze³³ observed that the adsorption enthalpy on soils changed by $-41 \text{ kJ}\cdot\text{mol}^{-1}$ per aromatic ring, and others have determined a value of $-40 \text{ kJ}\cdot\text{mol}^{-1}$ for the adsorption of benzene on an oven-dried soil.³⁴ The entropy of adsorption for benzene vapor on a dry surface is $(-73 \pm 1) \text{ J}\cdot\text{mol}^{-1}\cdot\text{K}^{-1}$, whereas that for naphthalene vapor on the dry surface is $(-95 \pm 5) \text{ J}\cdot\text{mol}^{-1}\cdot\text{K}^{-1}$. For all three compounds, the enthalpies of adsorption at the gas–water interface are smaller than those for the adsorption on the dry gas–solid interface. The binding strength of aromatic species to a dry mineral

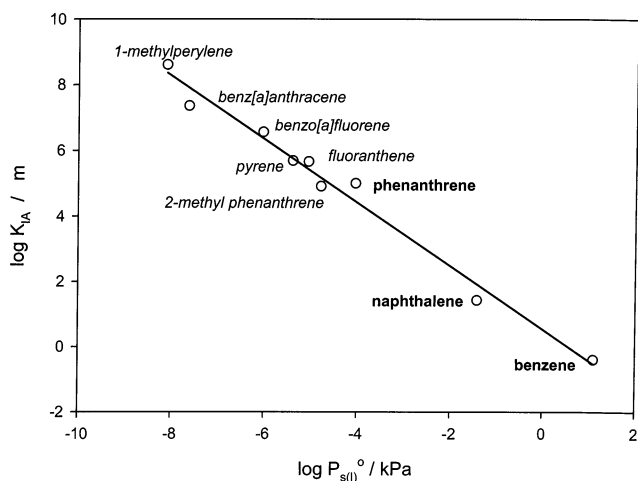


Figure 3. Correlation of $\log K_{IA}/\mu\text{m}$ with the log of the subcooled liquid vapor pressure, $P_{s(0)}^{\circ}/\text{kPa}$ ($r^2 = 0.983$). Compounds in bold are from this work. Data for the six additional compounds are obtained from other researchers.^{7,11}

surface is larger than that on the gas–water interface, and this may account for the smaller enthalpy of adsorption. This trend was also observed for the adsorption of PAHs on dry and wet soils.^{33,34}

A comparison of the free energy, enthalpy, and entropy of adsorption at the gas–solid interface with those at the gas–water interface can be made at a given temperature, viz. 298 K. It shows that for the PAH compounds the free energy value at the gas–solid interface is more negative than that at the gas–water interface, implying that the thermodynamics of adsorption is more favorable at the former interface. The enthalpy at the gas–solid interface is also more negative than that at the gas–water interface, indicating greater exothermic character at the former interface. However, the entropy of adsorption is distinctly more negative at the gas–water interface than at the gas–solid interface. In other words, there is a greater degree of freedom (mobility) for the adsorbed molecule at the gas–solid interface than that for the gas–water interface.

Previous work by Pankow³ showed that, within a given class of organic compounds, the value of K_{IA} is correlated with the subcooled liquid vapor pressure, $P_{s(0)}^{\circ}$. To do so, Pankow³ estimated the values of K_{IA} from experiments on the variation in adsorption of several PAHs on clean dry quartz surfaces as a function of relative humidity. By extrapolation of the data to 100% relative humidity, where a mineral surface will be covered by several monolayers of water, he estimated the values of K_{IA} and showed that, for 2 orders of magnitude in the vapor pressure of pure subcooled liquid, there exists a linear relationship with K_{IA} . Gustafsson and Gschwend¹¹ reported the water-to-interface partitioning, K_{IW} , of 1-methylperylene, another PAH. We converted K_{IW} to K_{IA} using the relationship $K_{IA} = K_{IW}/K_{AW}$ and obtained a value of $4.1 \times 10^8/\mu\text{m}$. We included our data from this work that extends the range of subcooled liquid vapor pressure to 9 orders of magnitude and plotted the K_{IA} versus $P_{s(0)}^{\circ}$; this is shown in Figure 3. Excellent correlation with $r^2 = 0.983$ confirms the correlation provided by Pankow.³ The new correlating equation is

$$\log(K_{IA}/\mu\text{m}) = -0.965 \log(P_{s(0)}^{\circ}/\text{kPa}) + 0.544$$

where K_{IA} is in micrometers and $P_{s(0)}^{\circ}$ is in kilopascal. This correlation will be helpful in estimating K_{IA} values for those compounds for which the experimental partition constants are not as such available. The fact that our experimental

values using the IGC technique are in line with the estimates by Pankow,³ who used a different methodology, is proof that both methods are capable of obtaining accurate values of K_{IA} . It should be noted that this correlation is not universal but applies only to PAHs; and as pointed out by Goss,⁴³ other factors such as acceptor and donor parameters must be considered for the adsorption of compounds that are ionic or polar in nature.

Implications for Atmospheric Deposition. A number of field measurements have shown that significant fractions of hydrophobic organic compounds (PAHs, pesticides) are associated with atmospheric fog droplets and ice surfaces.^{45–49} Deviations from Henry's law of gas–water partitioning have been observed. The presence of colloids or cosolvents in fogwater cannot reasonably account for this behavior.²⁶ An intriguing suggestion is that the large variation in size and the large gas–water interfacial area of fog droplets may account for the deviation.^{25,26} This assertion is based on earlier work by a number of investigators that shows that large differences between average compositions of fog droplets of varying sizes are observable.^{50–52} The results on gas–water interfacial partitioning presented in this paper allow an estimation of the effect of the large gas–water interfacial area on PAH concentration in fog.

Consider a fixed volume (V_F) of a foggy atmosphere containing n_0 moles of a PAH, of which n_w moles are “truly” dissolved in the bulk liquid water or associated with organic carbon in water, n_σ moles exist adsorbed to the gas–liquid interface, and n_a moles are in the gas phase. If the liquid volume fraction of the fog is $L = V_W/V_F$ and the gas–water interfacial area per liquid volume is $a_w/L = A_W/V_F = 6/d_p$, then the total scavenging efficiency (ϵ) is given by

$$\epsilon = \frac{n_w + n_\sigma}{n_0} = \frac{1}{1 + \frac{1}{LR_H K_{WA}}} \quad (6)$$

where $R_H = 1 + (6/d_p)(K_{IA}/K_{WA})$. Note that R_H represents the deviation from the conventional Henry's law partition constant between the bulk atmosphere and the fog droplet and d_p is the average droplet diameter. Note that if K_{IA} is very small or if d_p is very large, the surface adsorption is negligible ($R_H \rightarrow 1$) and the scavenging is solely by the bulk aqueous phase and is given by $\epsilon_0 = [1 + 1/LK_{WA}]^{-1}$. For molecules with large K_{IA} values, the increased surface effects will become evident only at low fog droplet diameters. Fog droplets are approximately $10 \mu\text{m}$ in average diameter, and the fogwater content, L , is approximately 10^{-6} . The difference between ϵ and ϵ_0 is large for a highly hydrophobic compound. For example, for pyrene, if surface adsorption is neglected, ϵ_0 is 2.2×10^{-3} , whereas when it is included, the value for a $10 \mu\text{m}$ droplet is $\epsilon = 0.22$. Thus, 3 orders of magnitude differences are observed. However, for a less hydrophobic compound such as benzene, there is little difference between the two estimates. Note that, in general, the ranges of scavenging efficiencies⁵³ for gaseous nonreactive species (nitrogen, oxygen, methane) in the atmosphere are from 10^{-8} to 10^{-6} , while only for reactive species (formaldehyde, hydrogen peroxide, etc.) will the value be higher, ≈ 0.1 . Thus, even for nonreactive species such as PAHs, the scavenging efficiency can approach those of reactive species at large gas–water interfacial areas. The concentrations in the fog droplet will depend on the product ϵx_0 , where x_0 is the mixing ratio of the substance in the gas phase.⁵³ Thus, compounds which have small mixing

ratios, such as pyrene, can still be scavenged appreciably in a foggy atmosphere if the droplet sizes are small so that ϵ is large.

Pandis and Seinfeld⁵¹ showed that when droplets of different properties (e.g. pH) but individually in equilibrium with the surrounding air are mixed, the resulting bulk solution is supersaturated with weak acids. This was attributed to the different Henry's law equilibrium relationships for different droplet samples. In the present case, different droplet sizes can lead to different equilibrium relationships (K dependent on d_p), and hence, the final fogwater sample will show large differences in overall solute concentration in water if one incorrectly assumes the equilibrium relationship (Henry's law) only between the bulk mixture and the original air phase. Compounds that have small Henry's constant, K_{WA} , but large K_{IA} will deviate considerably from the bulk phase relationship, especially if the droplet size d_p is small. Therefore, the expected deviation will be minimal for benzene as compared to a high molecular weight, low vapor pressure compound such as pyrene. Further experiments are being currently undertaken to test the hypothesis under both controlled laboratory conditions and natural field conditions in the metro Baton Rouge area.

Literature Cited

- Seinfeld, J. H.; Pandis, S. N. *Atmospheric Chemistry and Physics*, 2nd ed.; John Wiley & Sons: New York, 2000.
- Valsaraj, K. T. Hydrophobic Compounds in the Environment: Adsorption Equilibrium at the Air–Water Interface. *Water Res.* **1994**, *28*, 819–830.
- Storey, J. M. E.; Lo, W.; Isabelle, L. M.; Pankow, J. F. Gas/solid Partitioning of Semivolatile Organic Compounds to Model Atmospheric Solid Surfaces as a Function of Relative Humidity. 1. Clean Quartz. *Environ. Sci. Technol.* **1995**, *29*, 2420–2428.
- Saxena, P.; Hildemann, L. M. Water-Soluble Organics in Atmospheric Particles: A Review of the Literature and Application of Thermodynamics to Identify Candidate Compounds. *J. Atmos. Chem.* **1996**, *24*, 57–109.
- Bernstein, M. P.; Sandford, S. A.; Allamandola, L. J. Life's Far-Flung Materials. *Sci. Am.* **1999**, *281*, 42–49.
- Subramanyam, V.; Valsaraj, K. T.; Reible, D. D.; Thibodeaux, L. J. Gas-to-Particle Partitioning of PAHs in an Urban Atmosphere. *Atmos. Environ.* **1994**, *28*, 3083–3091.
- Pankow, J. F. Partitioning of Semi-volatile Organic Compounds to the Air/Water Interface. *Atmos. Environ.* **1997**, *31*, 927–929.
- Valsaraj, K. T. On the Physicochemical Aspects of Partitioning of Nonpolar Hydrophobic Organics at the Air–Water Interface. *Chemosphere* **1988**, *17*, 857–887.
- Valsaraj, K. T. Binding Constants for Non-Polar Hydrophobic Organics at the Air–Water Interface: Comparison of Experimental and Predicted Values. *Chemosphere* **1988**, *17*, 2049–2053.
- Goss, K. U. Adsorption of Organic Vapors on Polar Mineral Surfaces and on a Bulk Water Surface: Development of an Empirical Predictive Model. *Environ. Sci. Technol.* **1994**, *28*, 640–645.
- Gustafsson, O.; Gschwend, P. M. Hydrophobic Organic Compound Partitioning from Bulk Water to the Water/Air Interface. *Atmos. Environ.* **1999**, *33*, 163–165.
- Cutting, C. L.; Jones, D. C. Adsorption of Insoluble Vapors on Water Surfaces. Part I. *J. Chem. Soc.* **1955**, *77*, 4067–4075.
- Jones, D. C.; Ottewill, R. H. Adsorption of Insoluble Vapors on Water Surfaces. Part II. *J. Chem. Soc.* **1955**, *77*, 4076–4088.
- Blank, M.; Ottewill, R. H. The Adsorption of Aromatic Vapors on Water Surfaces. *J. Phys. Chem.* **1964**, *68*, 2206–2031.
- Hauxwell, F.; Ottewill, R. H. The Adsorption of Toluene Vapors on Water Surfaces. *J. Colloid Interface Sci.* **1968**, *28*, 514–521.
- Jho, C.; Nealon, D.; Shogbola, S.; King, A. D. Effect of pressure on the Surface Tension of Water: Adsorption of Hydrocarbon Gases and Carbon Dioxide on Water at Temperatures between 0 and 50 °C. *J. Colloid Interface Sci.* **1977**, *65*, 141–154.
- Karger, B. L.; Castells, R. C.; Sewell, P. A.; Hartkopf, A. Study of the Adsorption of Insoluble and Sparingly Soluble Vapors at the Gas–Liquid Interface of Water by Gas Chromatography. *J. Phys. Chem.* **1971**, *75*, 3870–3879.
- Karger, B. L.; Sewell, P. A.; Castells, R. C.; Hartkopf, A. Gas Chromatographic Study of the Adsorption of Insoluble Vapors on Water. *J. Colloid Interface Sci.* **1971**, *35*, 328–339.
- Hartkopf, A.; Karger, B. L. Study of the Interfacial Properties of Water by Gas Chromatography. *Acc. Chem. Res.* **1973**, *6*, 209–216.
- Mmerekhi, B. T.; Hicks, J. M.; Donaldson, D. J. Adsorption of Atmospheric Gases at the Air–Water Interface. *J. Phys. Chem. A* **2000**, *104*, 10789–10793.
- Nathanson, G. M.; Fsvidovits, P.; Worsnop, D. R.; Kolb, C. E. Dynamics and Kinetics at the Gas–Liquid Interface. *J. Phys. Chem.* **1996**, *100*, 13007–13020.
- Davidovits, P.; Hu, J. H.; Worsnop, D. R.; Zahniser, M. S.; Kolb, C. E. Entry of Gas Molecules into Liquids. *Faraday Discuss.* **1995**, *100*, 65–82.
- Mackay, D.; Shiu, W. Y.; Valsaraj, K. T.; Thibodeaux, L. J. Air–water transfer, the role of partitioning. In *Air–Water Mass Transfer*, 2nd Int. Symp.; Wilhelm, S. C., Gulliver, J. S., Eds.; ASCE: New York, 1990; pp 34–56.
- Hoff, J. T.; Mackay, D.; Gillham, R.; Shiu, W. Y. Partitioning of Organic Chemicals at the Air–Water Interface in Environmental Systems. *Environ. Sci. Technol.* **1993**, *27*, 2174–2180.
- Perona, M. J. The Solubility of Hydrophobic Compounds in Aqueous Droplets. *Atmos. Environ.* **1992**, *26A*, 2549–2533.
- Valsaraj, K. T.; Thoma, G. J.; Reible, D. D.; Thibodeaux, L. On the Enrichment of Hydrophobic Organic Compounds in Fog Droplets. *Atmos. Environ.* **1993**, *27*, 203–210.
- Costanza, M. S.; Brusseau, M. L. Contaminant Vapor Adsorption at the Gas–Water Interface of Soils. *Environ. Sci. Technol.* **2000**, *34*, 1–11.
- Pennell, K. D.; Rhue, R. D.; Rao, P. S. C.; Johnston, C. T. Vapor Phase Sorption of *p*-xylene and Water on Soils and Clay Minerals. *Environ. Sci. Technol.* **1992**, *26*, 756–763.
- Posner, A. M.; Anderson, J. R.; Alexander, A. E. The Surface Tension and Surface Potential of Aqueous Solutions of Normal Aliphatic Alcohols. *J. Colloid Interface Sci.* **1952**, *7*, 623–644.
- Ward, A. F. H. Thermodynamics of Monolayers on Solutions. I. The Theoretical Significance of Traube's Rule. *Trans. Faraday Soc.* **1946**, *42*, 399–417.
- Dorris, G. M.; Gray, D. G. Adsorption of Hydrocarbons on Silica-Supported Water Surfaces. *J. Phys. Chem.* **1981**, *85*, 3628–3635.
- Kemball, C.; Rideal, E. K. The Adsorption of Vapors on Mercury. I. Non-Polar Compounds. *Proc. R. Soc. (London)* **1946**, *A187*, 53–73.
- DeSeze, G. Sediment–Air Partitioning of Hydrophobic Organic Chemicals. Ph.D. Dissertation, Louisiana State University, 1999.
- Chiou, C. T.; Shoup, T. D. Soil Sorption of Organic Vapors and Effects of Humidity on Sorptive Mechanism and Capacity. *Environ. Sci. Technol.* **1985**, *19*, 1196–1200.
- Braunt, R. G.; Conklin, M. H. Dynamic Determination of Vapor/Water Interface Adsorption for Volatile Hydrophobic Organic Compounds (VHOCs) Using Axisymmetric Drop Shape Analysis: Procedure and Analysis of Benzene Adsorption. *J. Phys. Chem. B* **2000**, *104*, 11146–11152.
- Yaws, C. L. *Chemical Properties Handbook*; McGraw-Hill Publishing Co.: New York, 1999.
- Cabani, S.; Gianni, P.; Mollica, V.; Lepori, L. Group Contributions to the Thermodynamic Properties of Non-Ionic Organic Solutes in Dilute Aqueous Solution. *J. Solution Chem.* **1981**, *10*, 563–595.
- Valsaraj, K. T. *Elements of Environmental Engineering—Thermodynamics and Kinetics*, 2nd ed.; CRC Press: Boca Raton, FL, 2000.
- Dang, L. X.; Feller, D. Molecular Dynamics Study of Water–Benzene Interactions at the Liquid/Vapor Interface of Water. *J. Phys. Chem. B* **2000**, *104*, 4403–4407.
- Suzuki, S.; Green, P. G.; Bumgarner, R. E.; Dasgupta, S.; Goddard, W. A., III; Blake, G. A. Benzene Forms Hydrogen Bonds with Water. *Science* **1992**, *257*, 942–945.
- Orem, M. W.; Adamson, A. W. Physical Adsorption of Vapor on Ice. II. *n*-Alkanes. *J. Colloid Interface Sci.* **1969**, *31*, 278–286.
- Vidal-Madjer, C.; Guiochon, G.; Karger, B. L. Adsorption Potential of Hydrocarbons at the Gas–Liquid Interface of Water. *J. Phys. Chem.* **1976**, *80*, 394–402.
- Goss, K. U. Considerations about the Adsorption of Organic Molecules from the Gas Phase to Surfaces: Implications for Inverse Gas Chromatography and the Prediction of Adsorption Coefficients. *J. Colloid Interface Sci.* **1997**, *190*, 241–249.
- Donaldson, D. J.; Anderson, D. Adsorption of Atmospheric Gases at the Air–Water Interface. 2. C_1 to C_4 Alcohols, Acids, and Acetone. *J. Phys. Chem.* **1999**, *103*, 871–876.
- Glotfelty, D. E.; Majewski, M. S.; Seiber, J. N. Distribution of Several Organophosphorus Insecticides and their Oxygen Analogues in a Foggy Atmosphere. *Environ. Sci. Technol.* **1990**, *24* (4), 353–357.
- Capel, P. D.; Luenberger, C.; Giger, W. Hydrophobic Organic Chemicals in Urban Fog. *Atmos. Environ.* **1991**, *25*, 1335–1346.
- Aneja, V. P. Organic Compounds in Cloudwater and their Deposition at a Remote Continental Site. *J. Air Waste Manag. Assoc.* **1993**, *43*, 1239–1244.

- (48) Sagebiel, J. C.; Seiber, J. N. Studies on the Occurrence and Distribution of Wood Smoke Marker Compounds in Foggy Atmospheres. *Environ. Toxicol. Chem.* **1993**, *12*, 813–822.
- (49) Sokolov, O.; Abbatt, J. P. D. Adsorption to Ice of n-Alcohols (Ethanol to 1-Hexanol), Acetic Acid, and Hexanal. *J. Phys. Chem. A* **2002**, *106*, 775–782.
- (50) Pandis, S. N.; Seinfeld, J. H.; Pilinis, C. Chemical Composition Differences in Fog and Cloud Droplets of Different Sizes. *Atmos. Environ.* **1990**, *24A*, 1957–1969.
- (51) Pandis, S. N.; Seinfeld, J. H. Should Bulk Cloudwater or Fogwater Samples Obey Henry's Law? *J. Geophys. Res.* **1991**, *96* (D6), 10791–10798.
- (52) Munger, J. W.; Collett, J.; Daube, B.; Hoffmann, M. R. Chemical Composition of Coastal Stratus Clouds: Dependence on Droplet Size and Distance from the Coast. *Atmos. Environ.* **1989**, *23*, 2305–2320.
- (53) Warneck, P. *Chemistry of the Natural Atmosphere*, 2nd ed.; Academic Press: New York, 2000.

Received for review February 25, 2002. Accepted July 14, 2002. This work was supported by a grant from the National Science Foundation (ATM 0082836). F.S.Y. was supported through an REU supplement from NSF.

JE025520J